Polarizing beam splitter based on the anisotropic spectral reflectivity characteristic of form-birefringent multilayer gratings

Rong-Chung Tyan, Pang-Chen Sun, Axel Scherer,* and Yeshayahu Fainman

Department of Electrical and Computer Engineering, University of California, San Diego, La Jolla, California 92093

Received November 27, 1995

We introduce a novel polarizing beam splitter that uses the anisotropic spectral reflectivity (ASR) characteristic of a high-spatial-frequency multilayer binary grating. Such ASR effects allow us to design an optical element that is transparent for TM polarization and reflective for TE polarization. For normally incident light our element acts as a polarization-selective mirror. The properties of this polarizing beam splitter are investigated with rigorous coupled-wave analysis. The design results show that an ASR polarizing beam splitter can provide a high polarization extinction ratio for optical waves from a wide range of incident angles and a broad optical spectral bandwidth. © 1996 Optical Society of America

Polarizing beam splitters (PBS's) are essential components for numerous optical information processing applications such as free-space optical switching networks,[1] read–write magneto-optic data storage systems,[2] and polarization-based imaging systems.[3] These applications require that the PBS providing high extinction ratios tolerate a wide angular bandwidth and have a broad wavelength range and compact size for efficient packaging. Conventional PBS's employing either natural crystal birefringence (e.g., Wollaston prisms) or polarization selectivity of multilayer structures (e.g., PBS cubes) do not meet these requirements. The Wollaston prism requires a large thickness for generating enough walk-off distance between the two orthogonal polarizations, and PBS cubes provide good extinction ratios only in a narrow angular bandwidth for a limited wavelength range.[4]

In this Letter we introduce a new PBS device that uses the unique properties of anisotropic spectral reflectivity (ASR) characteristics of a high-spatial-frequency multilayer binary grating. The new ASR mechanism is based on combining the effects of the form birefringence of a high-spatial-frequency grating (i.e., the grating period is much less than the wavelength of the incident field) with the resonant reflectivity of a multilayer structure. We first describe intuitively the principle of ASR behavior by the use of effective medium theory (EMT).[5] Next we use rigorous coupled-wave analysis[6] tools for optimum design[7] of the PBS; the EMT results are used as an initial estimate. Finally, we characterize the ASR PBS in terms of polarization extinction ratio for operation with waves of wide angular bandwidth and broad wavelength range.

Consider a multilayer structure formed upon a substrate by deposition of alternating layers of dielectric materials with high and low indices of refraction, n_h and n_l, respectively. Such a structure exhibits high reflectivity in a wide spectral bandwidth, particularly when the thickness of each layer corresponds to a quarter-wave optical thickness for the center wavelength. One can increase the reflectivity of the quarter-wave structure by increasing the value of the ratio n_h/n_l and the number of layers. Larger values of n_h/n_l also increase the spectral bandwidth of high reflectance. For a multilayer structure made of isotropic dielectric materials, the reflectivity spectra for the two orthogonal linear polarizations at normal incidence are identical and therefore not easily separable. To separate them we need to substitute birefringent materials for one or both dielectric materials. Such a multilayer structure will possess reflectivity spectrum bands centered at different wavelengths for the two orthogonal polarizations, thereby providing the desired separation. However, multilayer structures consisting of natural anisotropic materials cannot be easily fabricated. Furthermore, since natural anisotropic materials possess very small birefringence [e.g., $(\Delta n/n)_{\mathrm{LiNbO_3}} \cong 0.03$ for a wavelength of 1.3 μm], this separation will be very limited. With our approach, the separation can be considerably increased because of the high anisotropy[8] that can be obtained with form birefringence.

Form birefringence effects[9] appear in high-spatial-frequency gratings formed by isotropic dielectric materials. Because of the geometric anisotropy of the grating structure, the two orthogonally polarized optical fields, one parallel to the grating grooves (designated the TE field) and the other perpendicular to the grating grooves (designated the TM field), encounter different effective dielectric constants and thus acquire a phase difference between them. This is similar to that obtained in natural anisotropic materials. Under normal incidence, the effective indices for the TE and TM polarizations of a surface-relief high-spatial-frequency binary grating can be estimated from the second-order EMT[5]:

$$n_{\mathrm{TE}}^{(2)} = \left[n_{\mathrm{TE}}^{(0)^2} + \frac{1}{3}\left(\frac{\Lambda}{\lambda}\right)^2 \pi^2 F^2 (1-F)^2 (n_{\mathrm{III}}^2 - n_{\mathrm{I}}^2)^2 \right]^{1/2}, \tag{1}$$

0146-9592/96/100761-03$10.00/0

$$n_{\mathrm{TM}}^{(2)} = \left[n_{\mathrm{TM}}^{(0)^2} + \frac{1}{3}\left(\frac{\Lambda}{\lambda}\right)^2 \pi^2 F^2 (1-F)^2 \times \left(\frac{1}{n_{\mathrm{III}}^2} - \frac{1}{n_{\mathrm{I}}^2}\right)^2 n_{\mathrm{TE}}^{(0)^2} n_{\mathrm{TM}}^{(0)^6} \right]^{1/2}, \quad (2)$$

where F is the duty cycle of the grating defined by $F = 1 - a/\Lambda$, where a is the width of the air gap in the grating (see Fig. 1), Λ is the grating period, λ is the wavelength of the incident wave, n_{I} and n_{III} are the indices of air and the grating material, respectively, and $n_{\mathrm{TE}}^{(0)} = [F n_{\mathrm{III}}^2 + (1-F) n_{\mathrm{I}}^2]^{1/2}$ and $n_{\mathrm{TM}}^{(0)} = \{n_{\mathrm{III}}^2 n_{\mathrm{I}}^2 / [F n_{\mathrm{I}}^2 + (1-F) n_{\mathrm{III}}^2]\}^{1/2}$ are the effective indices of refraction for TE and TM waves provided by the zero-order EMT, respectively.

Figure 1(a) shows an example of a high-spatial-frequency multilayer binary grating. We use SiO_2 and Si, with refractive indices of 1.45 and 3.51,[10] respectively (for a wavelength of 1.3 μm), as the two materials for the multilayer structures because of their fabrication compatibility and low absorption coefficients in the near-infrared region (this results in a low insertion loss). For operation of the form-birefringent grating in the zero diffraction order we set the grating period equal to 0.5 μm and the duty cycle to $F = 0.5$. Using second-order EMT equations (1) and (2) we obtain the following effective refractive indices for the two materials: $n_{\mathrm{TE,Si}}^{(2)} = 3.25$, $n_{\mathrm{TE,SiO_2}}^{(2)} = 1.26$ and $n_{\mathrm{TM,Si}}^{(2)} = 1.71$, $n_{\mathrm{TM,SiO_2}}^{(2)} = 1.18$. The effective indices of both materials are larger for TE polarization than for TM polarization. This means that in the spectral domain, the reflection band for TE polarization will be centered at a longer wavelength than that for TM polarization. We call this phenomenon ASR. This ASR characteristic is the essential property that one needs to realize the PBS.

Another characteristic is that the value of the effective index ratio for TE-polarized light $[(n_h/n_l)_{\mathrm{TE}} = 2.58]$ is larger than for TM-polarized light $[(n_h/n_l)_{\mathrm{TM}} = 1.45]$. This indicates that for the same reflectance the number of layers required by TE polarization will be less than that required by TM polarization. To minimize the number of layers needed to achieve a desired performance, we choose to maximize reflectivity for TE-polarized light. Therefore each layer has a quarter-wave optical thickness based on the TE effective index. These values, estimated by EMT, are used as the basis for a more accurate design that uses rigorous coupled-wave analysis. Optimization is done by incremental variation of the thickness of the layers to yield the highest extinction ratio at the operational wavelength of 1.3 μm. To achieve broad reflectance peaks in the spectrum, we use high-refractive-index materials for both the first and the last layers in the structure.

Figure 1(b) shows the numeric results of TE and TM reflectances as a function of the wavelength for a seven-layer high-spatial-frequency binary grating for normally incident optical fields. As expected, the TE polarization has a higher reflectance and broader bandwidth at a longer wavelength than the TM polarization. Such an ASR property cannot be accomplished with an isotropic multilayer structure for a normally incident optical field. The curves also show that the polarization extinct ratio remains high over a wide spectral range for the TM polarization. One can use these unique features in constructing polarization-selective mirrors for microlaser cavities or low-insertion-loss polarizer.

In order to separate the path of the reflected wave from that of the incident wave, we investigate a geometry in which the input wave vector is introduced at a 42° angle of incidence (lying in the plane perpendicular to the grating grooves and parallel to the grating vector). This slanted incidence arrangement possess two additional advantages: (1) Reflectivity from each layer for TE polarization is increased; thus we needed only five layers to achieve the desired performance (normal incidence required seven). (2) The sidelobe for the TM reflectivity is flattened, permitting operation of the beam splitter in a wider spectral range. Figure 2(b) shows the numerical results of the reflectance versus wavelength of the slanted incidence optical wave from the five-layer grating. For an incident wavelength of 1.3 μm, the TE and TM reflectances are 0.9971 and 0.0009128, respectively, and the polarization extinction ratio for reflection side of the beam splitter is better than 1100:1.

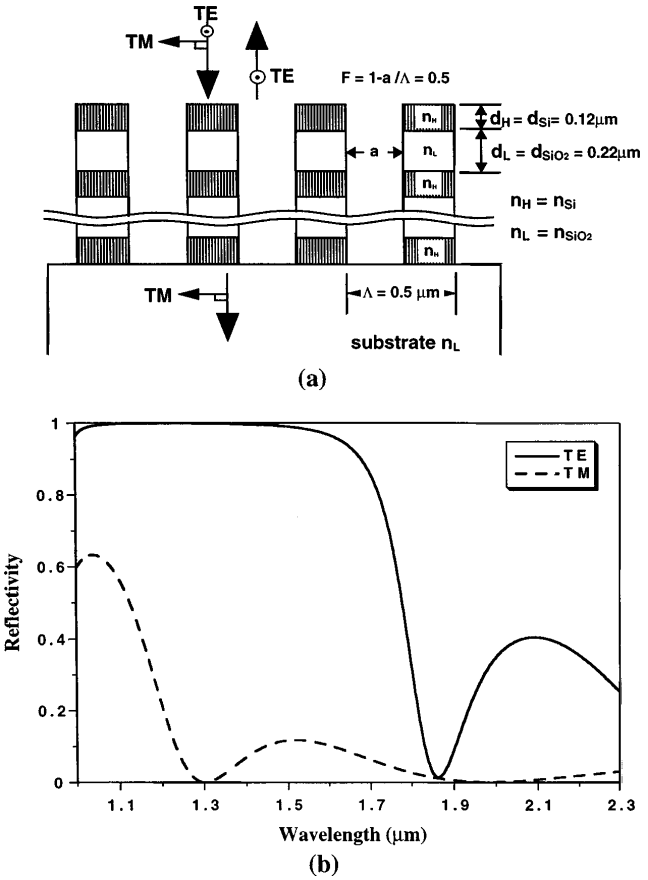

Fig. 1. (a) Schematic diagram of an ASR PBS operated with plane waves at normal incidence. (b) Numerical results of the reflectivity for TE- and TM-polarized waves versus wavelength of a seven-layer PBS designed for normally incident waves.

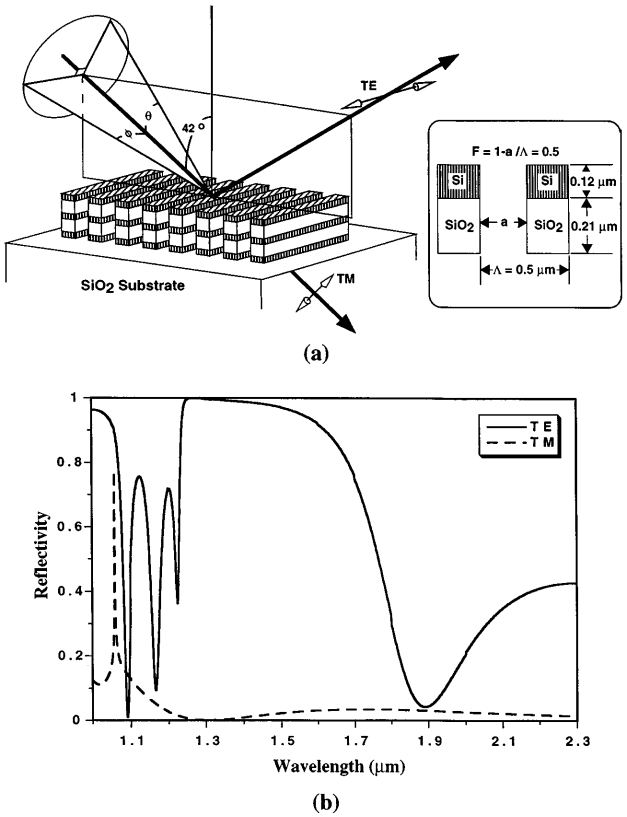

Fig. 2. (a) Schematic diagram of five-layer ASR PBS operated with incident waves at an angle of 42°. (b) Numerical results for the reflectivity of TE- and TM-polarized waves versus wavelength for 42° incidence.

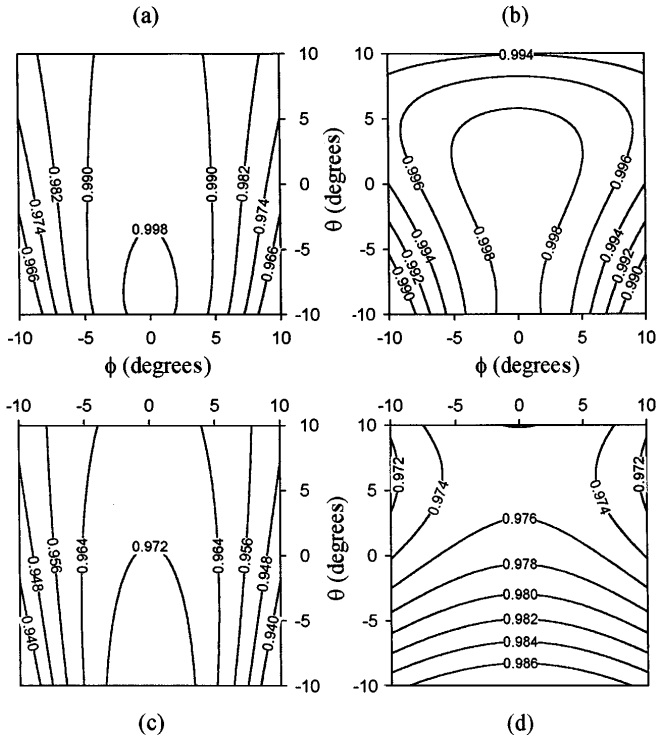

Fig. 3. Contour plots of TE reflectance and TM transmittance versus incident angles (ϕ, θ) as defined in Fig. 2(a): (a) TE reflectance at wavelength $\lambda = 1.3$ μm, (b) TM transmittance at wavelength $\lambda = 1.3$ μm, (c) TE reflectance at wavelength $\lambda = 1.5$ μm, and (d) TM transmittance at wavelength $\lambda = 1.5$ μm.

We also investigate the angular dependence of the ASR PBS. As shown in Fig. 2(a), the angles of incidence are varied to span an angular bandwidth of $\pm 10°$ in both the θ and the ϕ directions defined around the initial 42° bias angle. The results shown in Fig. 3 indicate that, at a wavelength of 1.3 μm, the reflectance for TE-polarized light and the transmittance for TM-polarized light are both better than 99% inside the 5° angular bandwidth cone and better than 97% inside the 10° angular bandwidth cone. Near 1.5 μm, results show that the TE reflectance and TM transmittance from this PBS are still better than 96% inside the 5° angular bandwidth cone and better than 94% inside the 10° angular bandwidth cone. These results show that a wide angular bandwidth as well as a broad spectral range of operation is possible with this design.

In conclusion, we have introduced a novel PBS device that is based on the ASR characteristic of a high-spatial-frequency multilayer binary grating. We use EMT for the initial design and rigorous coupled-wave analysis for optimization and numerical characterization of the ASR PBS. The results show that the ASR PBS's combine such unique features as small size, polarization selectivity for light at normal incidence, negligible insertion losses, high polarization extinction ratios, and operation with waves of large angular bandwidth and broad spectral range. These characteristics make these devices desirable for use in optical image processing, optical interconnections, and other polarization optics applications.

We thank Paul Shames and Fang Xu for helpful discussions and preparation of the manuscript. This research was supported in part by the National Science Foundation, the U.S. Air Force Office of Scientific Research, and the U.S. Air Force Rome Laboratory.

*Present address, Department of Electrical Engineering, California Institute of Technology, Pasadena, California 91125.

References

1. F. B. McCormick, F. A. P. Tooley, T. J. Cloonan, J. L. Brubaker, A. L. Lentine, R. L. Morrison, S. J. Hinterlong, M. J. Herron, S. L. Walker, and J. M. Sasian, Appl. Opt. **31,** 5431 (1992).
2. M. Ojima, A. Saito, T. Kaku, M. Ito, Y. Tsunoda, S. Takayama, and Y. Sugita, Appl. Opt. **25,** 438 (1986).
3. P. Kunstmann and H.-J. Spitschan, Opt. Commun. **4,** 166 (1971).
4. J. L. Pezzaniti and R. A. Chipman, Appl. Opt. **33,** 1916 (1994).
5. S. M. Rytov, Sov. Phys. JETP **2,** 466 (1956).
6. M. G. Moharam and T. K. Gaylord, J. Opt. Soc. Am. **72,** 1385 (1982).
7. I. Richter, P. C. Sun, F. Xu, and Y. Fainman, Appl. Opt. **34,** 2421 (1995).
8. F. Xu, R.-C. Tyan, P.-C. Sun, Y. Fainman, C.-C. Cheng, and A. Scherer, Opt. Lett. **20,** 2457 (1995).
9. M. Born and E. Wolf, *Principles of Optics* (Pergamon, Oxford, 1975), p. 705.
10. D. F. Edwards, in *Handbood of Optical Constants of Solids*, E. D. Palik, ed., (Academic, Orlando, Fla., 1985), p. 547.